

## Transient electronic structure of the photoinduced phase of $\text{Pr}_{0.7}\text{Ca}_{0.3}\text{MnO}_3$ probed with soft x-ray pulses

M. Rini,<sup>1</sup> Y. Zhu,<sup>1</sup> S. Wall,<sup>2</sup> R. I. Tobey,<sup>2,3</sup> H. Ehrke,<sup>2,3</sup> T. Garl,<sup>3</sup> J. W. Freeland,<sup>4</sup> Y. Tomioka,<sup>5</sup> Y. Tokura,<sup>5</sup> A. Cavalleri,<sup>2,3</sup> and R. W. Schoenlein<sup>1</sup>

<sup>1</sup>*Materials Sciences Division, Lawrence Berkeley National Laboratory, Berkeley, California, 94720 USA*

<sup>2</sup>*Department of Physics, University of Oxford, Oxford, OX1 3PU United Kingdom*

<sup>3</sup>*Max Planck Group for Structural Dynamics, University of Hamburg, CFEL, Hamburg 22607, Germany*

<sup>4</sup>*Advanced Photon Source, Argonne National Laboratory, Argonne, Illinois, 60439 USA*

<sup>5</sup>*Correlated Electron Research Center, AIST, Tsukuba Central 4, Tsukuba, Ibaraki 305-8562, Japan*

(Received 26 June 2009; published 7 October 2009)

We use time-resolved x-ray absorption near-edge structure spectroscopy to investigate the electronic dynamics associated with the photoinduced insulator-to-metal phase transition in the colossal magnetoresistive manganite  $\text{Pr}_{0.7}\text{Ca}_{0.3}\text{MnO}_3$ . Absorption changes at the O  $K$  and Mn  $L$  edges directly monitor the evolution of the density of unoccupied states in the transient photoinduced phase. We show that the electronic structure of the photoinduced phase is remarkably similar to that of the ferromagnetic metallic phase reached in related manganites upon cooling below the Curie temperature.

DOI: [10.1103/PhysRevB.80.155113](https://doi.org/10.1103/PhysRevB.80.155113)

PACS number(s): 78.47.jc, 71.30.+h, 75.47.Gk, 78.70.Dm

### I. INTRODUCTION

Since the discovery of the colossal negative-magnetoresistance effect (CMR), manganites have attracted considerable interest. In these materials, the application of a modest magnetic field can lead to the formation of a ferromagnetic metallic state, which, in some cases is inaccessible by temperature changes alone.<sup>1</sup> Recent evidence suggests that similar phenomena can be induced dynamically, either by photoexcitation<sup>2,3</sup> or by mode selective vibrational excitation.<sup>4,5</sup> Such a behavior may lead to new strategies for the realization of all-optical high-speed switches and data storage devices. However, our understanding of the underlying ultrafast mechanisms remains incomplete and a direct comparison between the dynamically induced phase and the CMR ferromagnetic-metallic state has never been performed. In the present work, we set out to understand the transient electronic structure of the photoinduced phase of the CMR perovskite  $\text{Pr}_{0.7}\text{Ca}_{0.3}\text{MnO}_3$ .<sup>1</sup> To this end, we use picosecond soft x-ray pulses from a synchrotron and time-resolved x-ray absorption near-edge structure (XANES) spectroscopy to sample the changes in the electronic density of states associated with the transient phase. We find a remarkable resemblance between photoinduced and temperature-induced changes in the XANES spectra, providing the direct evidence that the transient photoinduced phase has to be understood as the same electronic phase encountered in the CMR metallic state.

### II. STATIC XANES SPECTROSCOPY

Soft x-ray XANES spectroscopy is a powerful tool to investigate electronic, magnetic, and orbital configurations of complex oxides, probing the unoccupied part of the electronic structure of the system with symmetry selectivity and element specificity. This is especially important in manganites, in which valence and conduction bands and the ensuing conductive and magnetic properties are determined by the

hybridization of Mn  $3d$  shells and  $p$  states of bridging oxygen ligands.<sup>6,7</sup> Thus, complementary information can be obtained from XANES measurements in the spectral regions of the O  $K$  and Mn  $L$  edges which preferentially probe bands of  $p$  and  $d$  characters, respectively.

A scheme of the  $3d$  electronic structure of  $\text{Pr}_{0.7}\text{Ca}_{0.3}\text{MnO}_3$  is shown in Fig. 1(a). The key structural unit is the octahedral oxygen cage surrounding the transition metal ion. CMR manganites are mixed-valence oxides in which doping (Pr/Ca) results in a network of  $\text{Mn}^{3+}$  and  $\text{Mn}^{4+}$  ions. Electron hopping occurs between  $3d-e_g$  levels of neighboring  $\text{Mn}^{3+}$  and  $\text{Mn}^{4+}$  species and is favored by superexchange interactions via O  $2p$  states.<sup>6</sup> The unoccupied part of such electronic configurations is probed by XANES measurements.<sup>7</sup> The static XANES absorption spectra of  $\text{Pr}_{0.7}\text{Ca}_{0.3}\text{MnO}_3$  shown in Fig. 1(b) are measured at the 4-ID-C undulator beamline of the Advanced Photon Source at Argonne National Laboratory. Spectra were taken via total fluorescence yield (TFY) and total electron yield (TEY) with an energy resolution better than 0.25 eV. The agreement between TEY and TFY measurements at the O  $K$  edge confirms that reliable spectra can be taken in the more surface-sensitive TEY mode.

The oxygen  $K$  edge spectrum results from transitions between O  $1s$  core-level states and excited states with oxygen  $p$  character. The three-peak structure shown in Fig. 1(b) arises from covalent hybridization between O  $2p$  and unoccupied metal orbitals, as typically found in transition metal perovskites.<sup>8-10</sup> The features at 529.5, 536.5, and 543 eV are due to the hybridization with Mn  $3d$ , Pr  $5d$ /Ca  $3d$ , and Mn  $4sp$ /Pr  $6sp$  states, respectively.<sup>8-10</sup> This assignment is consistent with experimental studies on a series of manganese oxides with different oxidation states<sup>9</sup> and with band-structure calculations.<sup>10,11</sup> Via the Mn-O hybridization, the pre-edge peak at 529.5 eV [marked by a box in Fig. 1(b)] monitors electronic states of Mn  $d$  character close to  $E_F$ .<sup>8</sup> It thus carries the most interesting information about changes in the Mn-O hybridization that control  $d$ -electron conduc-

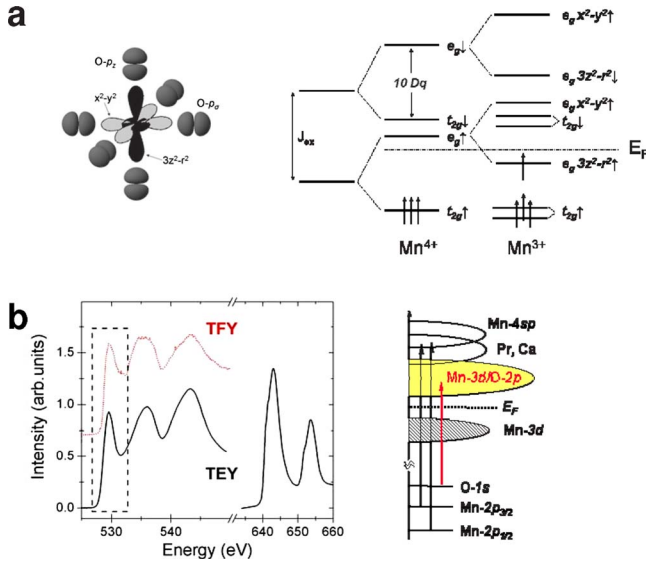


FIG. 1. (Color online) Electronic structure of  $\text{Pr}_{0.7}\text{Ca}_{0.3}\text{MnO}_3$ . (a) Sketch of the  $\text{MnO}_6$  octahedral geometry with relevant O  $2p$  and Mn  $3d$   $e_g$  orbitals. The scheme of the Mn  $d$  electronic structure is shown for  $\text{Mn}^{3+}$  and  $\text{Mn}^{4+}$  ions. The crystal field splitting ( $10Dq$ ) separates  $t_{2g}$  from  $e_g$  levels and strong exchange interaction aligns electron spins at a given atomic site. Electron hopping occurs between  $3d$ - $e_g$  levels of neighboring  $\text{Mn}^{3+}$  and  $\text{Mn}^{4+}$  species. In the  $\text{Mn}^{3+}$  ion, Jahn-Teller distortions lift the degeneracy of  $t_{2g}$  and  $e_g$  levels.  $\uparrow$  and  $\downarrow$  indicate majority and minority spins, respectively. (b) XANES spectra at the O  $K$  edge (530–550 eV), measured via total electron yield (TEY, solid curve) and total fluorescence yield (TFY, dotted curve), and at the Mn  $L_3$  and  $L_2$  edges (640–660 eV) measured in TEY mode at room temperature. A schematic of the electronic transitions contributing to O  $K$  and Mn  $L$  XANES spectra is shown.

tion. The O pre-edge derives from holes in an unresolved set of  $e_g^\uparrow$ ,  $t_{2g}^\uparrow$ , and  $e_g^\downarrow$  states.<sup>11</sup> The low-energy side at 529 eV corresponds to a transition to an unoccupied  $e_g^\uparrow$  state of the crystal-field-split  $\text{MnO}_6$  octahedra. The assignment of the main peak at 529.5 eV is still a matter of controversy.<sup>12–14</sup> Most authors emphasize the  $t_{2g}^\uparrow$  character, although  $e_g^\uparrow$  states may also contribute significantly<sup>12–14</sup> [see Fig. 1(a)].

The 640–660 eV spectral region in Fig. 1(b) represents the Mn  $L_{2,3}$  edges of the XANES spectrum of  $\text{Pr}_{0.7}\text{Ca}_{0.3}\text{MnO}_3$  measured via TEY at room temperature. This range directly probes excitations from  $2p$  core levels into unoccupied Mn  $3d$  states.<sup>15</sup> The two features at 643 and 654 eV are due to resonant excitation of the spin-orbit-split  $2p_{3/2}$  and  $2p_{1/2}$  core levels, approximately separated by the spin-orbit splitting of the Mn  $2p$  core hole. While the O  $1s$  pre-edge maps more directly the unoccupied electronic structure at the metal site, Mn- $L$ -edge spectra are dominated by multiplet effects stemming from Coulomb and exchange interactions between final-state  $2p$  core holes and  $3d$  electrons.<sup>16</sup> Multiplet calculations in the crystal octahedral symmetry provide a good description of the Mn  $L$  edges and allow extracting complementary information about the crystal-field interactions and the ground-state  $3d$  configuration.<sup>16</sup>

### III. TIME-RESOLVED XANES SPECTROSCOPY

Optical pump-XANES probe experiments are carried out on single-crystal  $\text{Pr}_{0.7}\text{Ca}_{0.3}\text{MnO}_3$  samples at 80 K, at beamline 6.0.2 at the Advanced Light Source of the Lawrence Berkeley National Laboratory. Transient XANES measurements are performed in a noncollinear pump-probe geometry, with a crossing angle of  $20^\circ$  between pump and probe beams. Samples are excited by 100 fs laser pulses at 1.5 eV ( $\lambda=800$  nm, penetration depth=200 nm). Photoinduced x-ray absorption changes are probed by delayed x-ray pulses tuned through the O- $K$ -edge and the Mn- $L$ -edge spectral regions. No polarization effects are observed in this pseudocubic system. X-ray absorption spectra are measured in TEY mode using a channeltron detector. The probing depth of TEY in this spectral region is on the order of several tens of angstroms. The experiment utilizes x-ray radiation from a single *camshaft pulse*, which is synchronized with the 1.5 eV pump pulse. The fast response of the channeltron detector allows isolating the camshaft pulse by means of electronic gating. The experimental time resolution is set by the 70 ps temporal width of the x-ray pulses. Monochromatic x rays are selected by a spectrometer with an energy resolution of  $\sim 0.5$  eV throughout this spectral region. A mechanical chopper running at 2 kHz is placed before the monochromator to reduce the x-ray flux.

Figure 2 compares the XANES spectra of the unexcited sample (laser off, solid circles) with spectra measured 300 ps after laser excitation at 1.5 eV (laser on, crosses). The spectra shown in Fig. 2 are taken at a pump fluence of  $20 \text{ mJ}/\text{cm}^2$ , above the threshold for inducing the transition to the metallic state.<sup>3</sup> Previous resistivity experiments under the same conditions have shown a drop in sample resistivity of six orders of magnitude, clearly indicating the formation of a metallic state at this pump fluence.<sup>3</sup> A large redshift of spectral weight is observed at the O  $K$  edge [Fig. 2(a)] and, to a lesser extent, at the Mn  $L$  edge [Fig. 2(b)]. Figures 2(c) and 2(d) show time-dependent pump-probe signals measured at the low-energy edges of the O (529 eV) and the Mn (540.5 eV) absorption resonances as a function of the delay time between laser and x-ray pulses. Solid lines are fit to the data using a cross correlation width of 70 ps, corresponding to the temporal resolution dictated by the x-ray pulse width.

### IV. RESULTS AND DISCUSSION

These results provide insights into the striking similarity between the photoinduced phase and the low-temperature metallic phase of CMR manganites. Previous time-resolved studies used two indirect approaches. First, femtosecond optical reflectivity was applied to probe ultrafast changes in the dielectric constant at visible or near-IR frequencies.<sup>17</sup> Second, transport measurement with nanosecond resolution monitored photoinduced conductivity changes.<sup>2</sup> Although the ultrafast formation of a lower-conductivity phase had been established, those studies could not directly compare the electronic structures and the conduction mechanisms of the two metallic phases (low temperature and photoinduced). Our XANES measurements prove that the photoinduced modifications of the Mn  $3d$  structure are identical to those

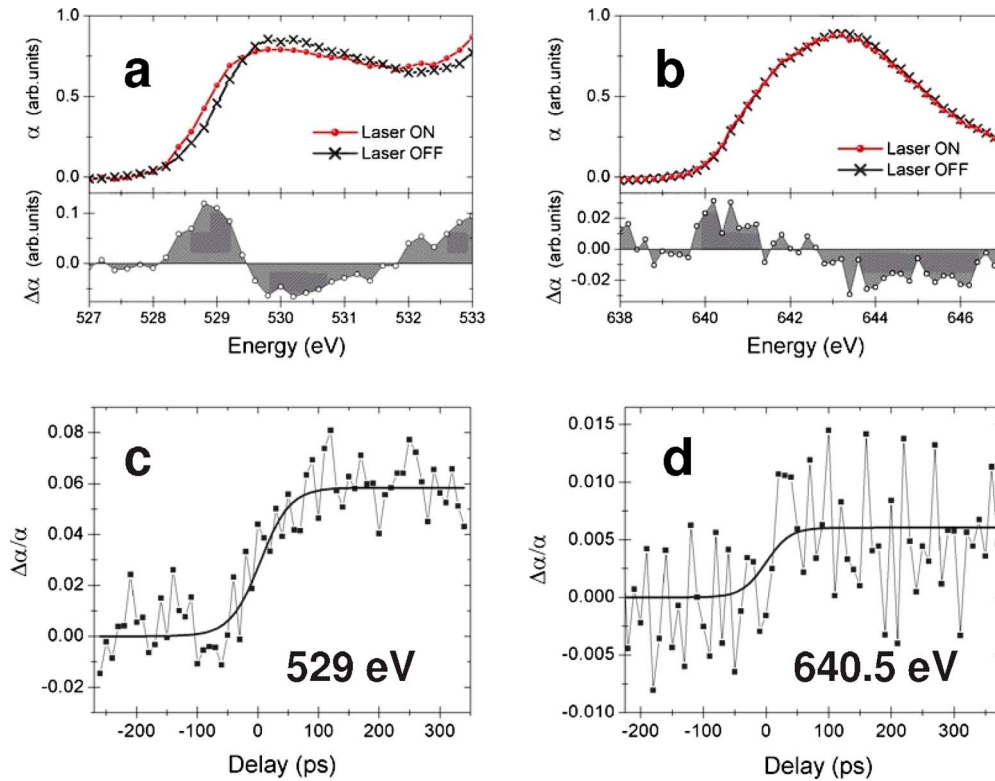


FIG. 2. (Color online) Time-resolved XANES measurements at O  $K$  and Mn  $L$  edges. Static absorption spectra (solid circles) at the (a) O  $K$  pre-edge and (b) Mn  $L_3$  edge and spectra measured 300 ps after 800 nm excitation (crosses). Lower panels: corresponding relative change in absorption ( $\Delta\alpha/\alpha$ ). (c) and (d) Relative change in absorption ( $\Delta\alpha/\alpha$ ) as a function of pulse delay at two representative wavelengths, 529 (O  $K$  edge) and 640.5 eV (Mn  $L$  edge). The solid line is a fit of the data using a cross correlation width of 70 ps, corresponding to the temporal resolution of the experiment. Measurements were taken at 80 K via TEY.

occurring upon the formation of the low temperature ferromagnetic, metallic phase.

Our time-resolved O- $K$ -edge spectra reveal photoinduced absorption changes that are very similar to those observed in related manganites exhibiting temperature-controlled phase transitions. As shown by temperature-dependent XANES studies in a broad class of CMR compounds,<sup>7,13</sup> the formation of the metallic phase below the Curie temperature has unambiguous signatures in the O pre-edge absorption spectrum,<sup>7,13</sup> resulting from the electronic changes that accompany the insulator-metal transition<sup>13,14</sup> and from modifications in Jahn-Teller (JT) distortions.<sup>7,14</sup> In the insulating state, JT distortions lift the degeneracy of the  $e_g$  levels and thereby contribute to charge localization.<sup>6</sup> Temperature effects are not observable in  $\text{Pr}_{1-x}\text{Ca}_x\text{MnO}_3$ , a distorted perovskite with small electronic bandwidth, which does not order ferromagnetically and remains insulating at all temperatures and doping levels.<sup>1</sup> Figure 3 compares photoinduced absorption changes in  $\text{Pr}_{0.7}\text{Ca}_{0.3}\text{MnO}_3$  [Fig. 3(a)] at the O  $K$  edge with temperature-induced absorption changes observed in perovskite and double-layered manganites within a broad range of electronic bandwidths and critical temperatures: the perovskite manganites  $\text{La}_{0.7}\text{Sr}_{0.3}\text{MnO}_3$  [ $T_C=360$  K, Fig. 3(b)] and  $\text{Pr}_{0.7}\text{Sr}_{0.3}\text{MnO}_3$  [ $T_C=250$  K, Fig. 3(c)] and the double-layered compound  $\text{La}_{1.3}\text{Sr}_{0.7}\text{Mn}_2\text{O}_7$  [ $T_C=130$  K, Fig. 3(d)]. Absorption changes for the temperature-induced case are measured as the difference between absorption below the critical temperature  $T_C$  (metallic phase) and absorption above

$T_C$  (insulating phase). Data for Figs. 3(b)–3(d) are taken from Refs. 7 and 13 and convolved with a spectral resolution of 0.5 eV for a direct comparison with the time-resolved XANES spectra. In both the photoinduced and the thermally induced phase transitions, remarkably similar features are observed. The edge of the oxygen absorption redshifts by 0.2 eV and the differential spectra exhibit a 0.7 eV broad peak at the pre-edge absorption threshold. Such width has been related to the expected O  $1s$  core-hole lifetime broadening typical of transition metal oxides.<sup>13</sup>

Following the analysis carried out for temperature-dependent studies,<sup>7,13,14</sup> the dynamics of time-resolved XANES spectra can be connected to rearrangements of the density of states across the insulator-metal transition. As the metallic state is formed and the insulating band gap collapses, the density of  $e_g^\dagger$  unoccupied states in the conduction band changes and builds up near  $E_F$ . Since the O  $K$  edge directly maps electronic Mn  $d$  states close to  $E_F$ , this results in a transfer of spectral weight to the absorption threshold.<sup>13</sup> As discussed by Toulemonde *et al.*,<sup>7</sup> the reduction in the strong dynamic Jahn-Teller distortions may also contribute to the observed absorption changes. As the system turns metallic, the Jahn-Teller splitting of both  $e_g$  and  $t_{2g}$  sublevels is considerably reduced. This results in a clear  $e_g^\dagger$ - $t_{2g}^\dagger$  separation (see Fig. 1), which leads to the absorption changes shown in Fig. 3(c). Although the spectral resolution of the time-resolved XANES experiments is insufficient to resolve the  $e_g$

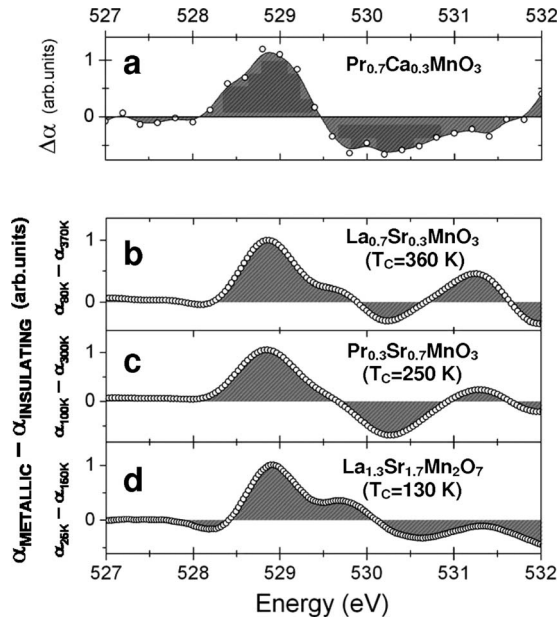


FIG. 3. Effect of insulator-metal transition on the prestructure of O-K-edge XANES spectra. Spectrally resolved changes in the O-K-edge XANES spectrum for (a) photoinduced phase transition in  $\text{Pr}_{0.7}\text{Ca}_{0.3}\text{MnO}_3$ ,  $\Delta\alpha = \alpha_{\text{METALLIC}} - \alpha_{\text{INSULATOR}} = \alpha(300 \text{ ps}) - \alpha(-300 \text{ ps})$ . (b)–(d) Temperature-induced phase transition in manganites,  $\Delta\alpha = \alpha_{\text{METALLIC}} - \alpha_{\text{INSULATOR}} = \alpha(T < T_C) - \alpha(T > T_C)$ . (b)  $\text{La}_{0.7}\text{Sr}_{0.3}\text{MnO}_3$ ,  $T_C = 360 \text{ K}$  (Ref. 15); (c)  $\text{Pr}_{0.3}\text{Sr}_{0.7}\text{MnO}_3$ ,  $T_C = 250 \text{ K}$  (Ref. 9); and (d) double-layered  $\text{La}_{1.3}\text{Sr}_{1.7}\text{Mn}_2\text{O}_7$ ,  $T_C = 130 \text{ K}$  (Ref. 15).

and the  $t_{2g}$  features, our data are consistent with this interpretation.

The observation of photoinduced changes at the Mn  $L$  edge is also important, since the band-gap collapse and the relaxation of Jahn-Teller distortions must directly affect the Mn  $3d$  states. The scale of the effect at the  $L$  edge is in agreement with static temperature-dependent studies,<sup>7</sup> which show much more subtle effects than at the O  $K$  edge. Upon cooling below  $T_C$ , small absorption changes are observed over a narrow spectral range at the low-energy edge of the Mn  $3d$  absorption.<sup>7</sup> However, the 0.5 eV spectral resolution of our experiments hinders a direct comparison with the temperature-driven transition.

Importantly, the observed photoinduced absorption changes reveal the nonthermal nature of the insulator-metal phase transition. The significant shift of spectral weight cannot be explained as a consequence of laser heating. On the 70 ps time scale accessible in these experiments, electron-lattice thermalization leads to a temperature increase of less than 100 K at the 20  $\text{mJ}/\text{cm}^2$  pump fluence. Figure 4(a) shows temperature-dependent XANES studies of the O-K-edge region measured in TFY mode over a broad temperature range. Temperature effects in this spectral region are much less pronounced than in the photoinduced case since in  $\text{Pr}_{0.7}\text{Ca}_{0.3}\text{MnO}_3$  an insulator-to-metal phase transition cannot be thermally induced.<sup>1</sup> Furthermore, photoinduced x-ray absorption changes exhibit threshold and saturation dependence on the pump fluence, characteristic of a phase

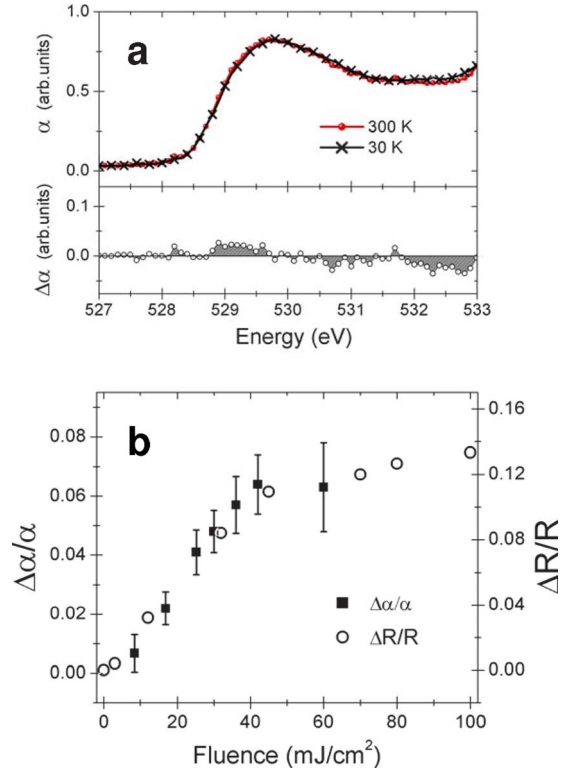


FIG. 4. (Color online) Evidence of a nonthermal phase transition. (a) Static absorption spectra at the O  $K$  edge measured via TFY at room temperature (solid circles) and 30 K (crosses). Lower panel: corresponding relative change in absorption ( $\Delta\alpha/\alpha$ ). (b) Fluence dependence of photoinduced relative absorption changes at 529 eV (solid squares) from XANES experiments and reflectivity changes at 1.5 eV (open circles), from optical pump-probe experiments (Ref. 3).

transformation.<sup>3</sup> Figure 4(b) compares the fluence dependence of photoinduced absorption changes at 529 eV (solid squares) and photoinduced reflectivity changes at 1.5 eV (open circles), as measured in optical pump-probe experiments.<sup>3</sup> XANES signals exhibit the same behavior as near-infrared reflectivity changes, which are related to the shift of Drude weight in optical conductivity resulting from the transition to the metallic state.

## V. CONCLUSIONS

In summary, time-resolved XANES spectroscopy is used to study the electronic structure of the photoinduced phase of the CMR manganite  $\text{Pr}_{0.7}\text{Ca}_{0.3}\text{MnO}_3$ . Absorption changes at the O  $K$  and Mn  $L$  edges directly monitor the evolution of the density of unoccupied of states in the transient photoinduced phase and clearly indicate that this phase is metallic. Furthermore, our results show that this transient metallic phase is not attributable to simple heating or increase in internal energy. Rather, the electronic structure of the photoinduced phase is strongly reminiscent of the metallic phase reached by cooling larger-bandwidth manganites below the Curie temperature. If the transient metallic state is understood to be a ferromagnetic phase stabilized by

double-exchange,<sup>6</sup> then the photoinduced phase transition in manganites may provide an intriguing path for the ultrafast optical control of magnetization. While ultrafast photoinduced melting of ferromagnetic order has been demonstrated in some metals,<sup>18</sup> the photoinduced transition in  $\text{Pr}_{0.7}\text{Ca}_{0.3}\text{MnO}_3$  is much more subtle. Here, the formation of a ferromagnetic state would imply ultrafast symmetry lowering of the magnetic system. Time-resolved x-ray dichroism studies will help to measure the magnetic response on ultrafast time scales and to identify elementary time scales and pathways for this process.

## ACKNOWLEDGMENTS

We thank Norman Mannella for helpful discussions and Nils Huse for experimental contributions. Work at Lawrence Berkeley National Laboratory was supported by the Department of Energy under Contract No. DE-AC02-05CH11231. Use of the Advanced Photon Source is supported by the U. S. Department of Energy, Office of Science, under Contract No. DE-AC02-06CH11357

- 
- <sup>1</sup>Y. Tomioka, A. Asamitsu, H. Kuwahara, Y. Moritomo, and Y. Tokura, *Phys. Rev. B* **53**, R1689 (1996).
- <sup>2</sup>K. Miyano, T. Tanaka, Y. Tomioka, and Y. Tokura, *Phys. Rev. Lett.* **78**, 4257 (1997).
- <sup>3</sup>D. Polli, M. Rini, S. Wall, R. W. Schoenlein, Y. Tomioka, Y. Tokura, G. Cerullo, and A. Cavalleri, *Nature Mater.* **6**, 643 (2007).
- <sup>4</sup>M. Rini, R. Tobey, N. Dean, J. Itatani, Y. Tomioka, Y. Tokura, R. W. Schoenlein, and A. Cavalleri, *Nature (London)* **449**, 72 (2007).
- <sup>5</sup>R. I. Tobey, D. Prabhakaran, A. T. Boothroyd, and A. Cavalleri, *Phys. Rev. Lett.* **101**, 197404 (2008).
- <sup>6</sup>M. Imada, A. Fujimori, and Y. Tokura, *Rev. Mod. Phys.* **70**, 1039 (1998).
- <sup>7</sup>O. Toulemonde, F. Millange, F. Studer, B. Raveau, J.-H. Park, and C.-T. Chen, *J. Phys.: Condens. Matter* **11**, 109 (1999).
- <sup>8</sup>M. Abbate, F. M. F. de Groot, J. C. Fuggle, A. Fujimori, O. Strebler, F. Lopez, M. Domke, G. Kaindl, G. A. Sawatzky, M. Takano, Y. Takeda, H. Eisaki, and S. Uchida, *Phys. Rev. B* **46**, 4511 (1992).
- <sup>9</sup>H. Kurata and C. Colliex, *Phys. Rev. B* **48**, 2102 (1993).
- <sup>10</sup>M. Abbate, G. Zampieri, F. Prado, A. Caneiro, and A. R. B. de Castro, *Solid State Commun.* **103**, 9 (1997).
- <sup>11</sup>M. K. Dalai, P. Pal, B. R. Sekhar, N. L. Saini, R. K. Singhal, K. B. Garg, B. Doyle, S. Nannarone, C. Martin, and F. Studer, *Phys. Rev. B* **74**, 165119 (2006).
- <sup>12</sup>E. Pellegrin, L. H. Tjeng, F. M. F. de Groot, R. Hesper, G. A. Sawatzky, Y. Moritomo, and Y. Tokura, *J. Electron Spectrosc. Relat. Phenom.* **86**, 115 (1997).
- <sup>13</sup>J.-H. Park, T. Kimura, and Y. Tokura, *Phys. Rev. B* **58**, R13330 (1998).
- <sup>14</sup>N. Mannella, A. Rosenhahn, M. Watanabe, B. Sell, A. Nambu, S. Ritchey, E. Arenholz, A. Young, Y. Tomioka, and C. S. Fadley, *Phys. Rev. B* **71**, 125117 (2005).
- <sup>15</sup>Y. S. Lee, V. G. Prokhorov, H. J. Shin, and Y. P. Lee, *Phys. Status Solidi A* **196**, 70 (2003).
- <sup>16</sup>F. M. F. de Groot, *Coord. Chem. Rev.* **249**, 31 (2005).
- <sup>17</sup>M. Fiebig, K. Miyano, Y. Tomioka, and Y. Tokura, *Appl. Phys. Lett.* **74**, 2310 (1999).
- <sup>18</sup>E. Beaurepaire, J.-C. Merle, A. Daunois, and J.-Y. Bigot, *Phys. Rev. Lett.* **76**, 4250 (1996).